energy&fuels

pubs.acs.org/EF
Article

Impact of Catalyst Quantity on Premixed Ultralean Hydrogen/Air Combustion in a Packed Bed Reactor

Md Nur Alam Mondal, Nader Karimi, S. David Jackson, and Manosh C. Paul*

Cite This: *Energy Fuels* 2025, 39, 9121−9133
Read Online

ABSTRACT: Catalytic combustion of an ultra-lean hydrogen/air mixture is a promising technique for generating heat with extremely low emissions, especially in low-temperature heating applications. A major challenge of this technique is the reliance on noble catalysts, which are both expensive and rare in nature. Therefore, minimizing the use of catalysts is essential for cost-effective catalytic combustion system designs. This work experimentally investigates the effects of varying catalyst contents and loadings in a packed bed tubular catalytic reactor. Active catalyst sites are applied to the surfaces of Al_2O_3 pellets that make up the packed bed. An ultra-lean premixed mixture of 2% H_2 by volume in air is used for the catalytic combustion. The catalyst contents tested include 0.3, 0.5, and 1.0% Pt in Pt/Al_2O_3 pellets and 0.5 and 5.0% Pd in Pd/Al_2O_3 pellets. Catalyst loadings for both catalyst pellets were set at 1.0 2.5, and 5.0 g. Measurements were taken in the packed bed reactor across the flow rates ranging from 1 to 5 LPM. The results show that the packed bed with higher Pt or Pd content generates elevated combustion temperatures and demonstrates an effective catalytic performance. Additionally, the occurrence of superadiabatic conditions was observed, and hydrogen conversion rates were significantly influenced by the catalyst contents. Notably, the pellets with high Pt or Pd content exhibited catalytic performance comparable to higher catalyst loadings at different flow conditions, even with a loading of 1 g at low flow rates. However, increasing the catalyst loading affects the reaction mechanism, shifting it from kinetic control to diffusion control.

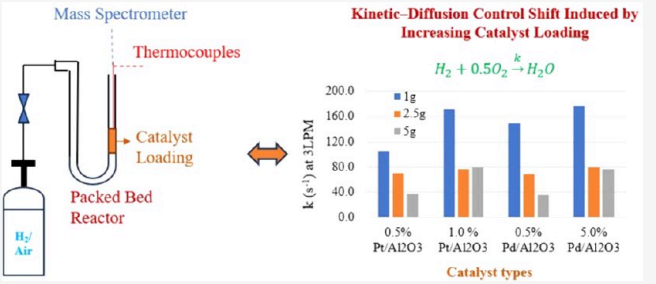

1. INTRODUCTION

Catalytic combustion is a well-established technique for heat generation systems, used in various applications.[1−3] In this technique, the catalyst facilitates the oxidation reaction without being consumed. The fundamental principles of catalytic combustion and its behavior across different reactor systems have been extensively reviewed in the literature.[4−6] Over the years, both experimental and numerical studies have advanced the understanding of catalytic processes.[7−9] Currently, innovations and advancements in catalytic combustion are rapidly evolving, particularly in integrating this technology into combustion systems such as gas turbines, furnaces, and boilers.[2,10,11]

One notable feature of catalytic combustion is its effectiveness in reducing NO_x emissions at low temperatures, and it has been used in engines for many years.[12,13] The mechanism of NO_x reduction using noble catalysts like platinum (Pt), rhodium (Rh), and palladium (Pd) has been reported in the literature.[14,15] Current research is exploring the combustion of hydrogen/air mixture with the presence of noble catalyst materials in reactors like honeycomb monolith, packed bed, and porous reactors, aiming to stabilize the flame and reduce NO_x.[6,16] Efforts are also made to utilize metal oxide and perovskite oxide catalysts for hydrogen combustion.[5,17] Transition metal oxides, such as those containing cobalt (Co), copper (Cu), manganese (Mn), and nickel (Ni), are inexpensive and demonstrate catalytic performance in hydrogen combustion that is comparable to that of noble metals.[18] However, these catalysts require preheating to initiate the catalytic combustion of hydrogen. Similarly, perovskite oxide catalysts are also cost-effective, featuring a unique structure that includes alkaline, rare earth elements like lanthanum (La), strontium (Sr), bismuth (Bi), and transitional metals.[17] Although some studies[19,20] have reported that perovskite catalysts exhibit effective catalytic activity in hydrogen combustion, they tend to have relatively low specific surface areas, which can lead to insufficient catalytic performance.

However, the use of catalysts in hydrogen combustion is significant for a wide range of operating conditions in various reactor applications. Because the conventional method of

Received: January 31, 2025
Revised: April 25, 2025
Accepted: April 28, 2025
Published: May 5, 2025

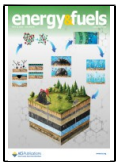

https://doi.org/10.1021/acs.energyfuels.5c00576
Energy Fuels 2025, 39, 9121−9133

hydrogen combustion can lead to several issues, including flashback, flame instability, hotspots, and incomplete combustion.[21−24] Additionally, achieving effective NO_x reduction without a catalyst in hydrogen flames across a wide range of operating conditions proves to be challenging, even with reactor design modifications. For instance, Yilmaz et al.[25] investigated the effects of geometry on NO_x emissions by examining various configurations, including a cavity, a backward-facing step, and multiple channels within the combustor using the hydrogen/air equivalence ratio of 0.8. They reported that NO_x levels varied across all configurations, ranging from 1.0×10^{-8} to 3.6×10^{-8} mass fraction at temperatures between 1300 and 1600 K. Similarly, Meraner et al.[26] studied the NO_x emission characteristics using a conical bluff body inside the hydrogen burner with an equivalence ratio ranging from 0.7 to 1.3. Their results indicated that dry NO_x levels varied from 60 to 90 ppm under different operating conditions and increased with thermal load. Moreover, NO_x characteristics were studied using a blend of hydrogen and methane in various reactor configurations.[27−29] For example, Boulahlib et al.[28] conducted experimental work on a multiflame burner designed for domestic boiler applications, where they experimented with blending hydrogen with methane at levels ranging from 0 to 45%. They reported the NO_x levels of 5−20 ppm at low flue gas temperatures ranging from 80 to 118 °C under different blending conditions. However, NO_x emissions can be greatly reduced with catalyst-aided combustion.[5] In a study focused on an ultralow NO_x burner, Fumey et al.[30] conducted an experimental investigation of a catalytic hydrogen burner using Pt-coated porous disks. They measured NO_x levels of 0.09 and 9.49 ppmv at hydrogen/air equivalence ratios of 0.33 and 0.66, respectively. Similarly, Mondal et al.[31] performed a numerical investigation of NO_x levels in a Pt-coated planar reactor and estimated NO_x emissions to be between 0 and 0.016 ppmv at equivalence ratios ranging from 0.10 to 0.20.

Catalytic combustion implemented in combustion systems, as illustrated in Figure 1, can be classified into two types: fuel-lean catalytic combustion (a) and fuel-rich catalytic combustion (b).[32] Fuel-lean catalytic combustion can further be divided into two subtypes: partial catalytic conversion (a1), where part of the fuel undergoes catalytic conversion and the remainder is combusted in the gas phase, and total catalytic conversion (a2), which is a purely catalytic process.[33] In fuel-rich catalytic combustion (b), catalytic conversion occurs under fuel-rich conditions and the unburned fuel is subsequently combusted in the gas phase with the help of bypass air. The selection of the appropriate catalytic combustion technique depends on the specific application and operating conditions.

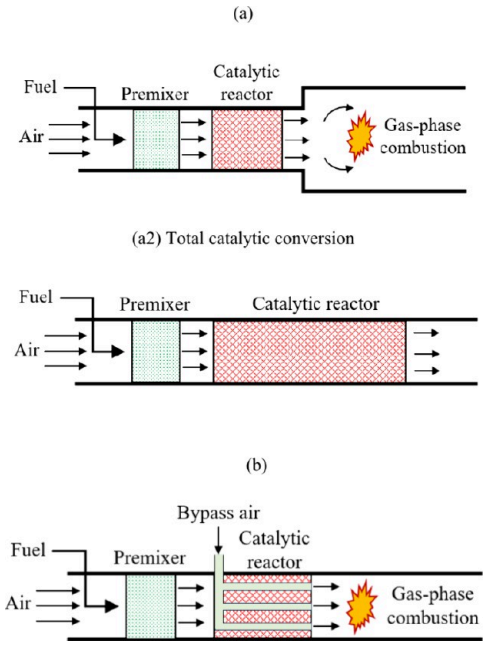

Figure 1. Catalytic combustion systems. (a) Fuel-lean catalytic conversion: (a1) partial catalytic conversion; (a2) total catalytic conversion. (b) Fuel-rich catalytic conversion.

However, total catalytic conversion under fuel-lean conditions is considered in this study, focusing on low-temperature heating applications. In such cases, the catalytic unit plays a critical role, as most catalysts used are noble metals, such as Pt, Pd, and Rh, which are expensive. Additionally, the catalytic performance is also essential, as it varies based on reactor design and catalyst loading.[34,35] Among the various catalytic reactor designs, monolithic and packed bed reactors are the most commonly used in catalytic combustion systems, as reported in the literature.[8,36−38] In a monolithic structure,[31] the catalyst is coated onto the surfaces of parallel channels, while in a packed bed reactor, the catalyst is applied to the surface of the pellets. Despite the differences in physical design, both types of reactors operate on similar principles, facilitating catalytic reactions by maximizing the contact area between the reactants and the catalyst.

However, hydrogen is becoming a key fuel for future heating systems; therefore, further research into catalyst utilization in hydrogen combustion systems is essential. The catalytic hydrogen combustion (eq 1) is a total oxidation reaction that occurs in the presence of an active catalyst, which controls both the apparent reaction rate constant and the activation energy.

$$H_2 + \frac{1}{2}(O_2 + 3.76N_2) \xrightarrow{\text{catalyst}} H_2O + 1.88N_2 \quad (1)$$

$$\text{reaction rate} = kC_{H_2} \text{ and } k = Ae^{-E_a/RT} \quad (2)$$

where C_{H_2}, k, and E_a are the hydrogen concentration, apparent reaction rate constant, and activation energy, respectively. The potential of hydrogen catalytic combustion with extremely low NO_x emissions for fuel ultralean to lean conditions is reported in a number of studies.[31,32,39] Moreover, catalytic combustion at low temperatures suppresses gas-phase combustion, eliminates the risk of flashback, and enhances the overall safety of the system.[35,38] Therefore, an ultralean hydrogen/air mixture is chosen for catalytic analysis in the present work. The catalytic reactor considered for investigation is a catalyst-packed bed type. Because this is easier to build, cheaper, and more practical than a catalytic monolith reactor for experimental investigation. The catalyst-packed bed reactor has been investigated for many years, focusing on the size and shape of the catalyst pellet, packed bed length and catalyst materials in the catalytic process.[40−43] Furthermore, studying catalytic combustion with minimal catalyst usage is crucial for ensuring cost-effectiveness and broadening its applicability. This aspect is not extensively explored in the literature, particularly the effect of catalyst amount on fuel ultralean combustion. Therefore, it necessitates experimental investigation to understand how the catalyst quantity influences the catalytic combustion process. Previous studies[44−46] on catalytic packed bed reactors have been largely numerical, with limited experimental data available on the

https://doi.org/10.1021/acs.energyfuels.5c00576
Energy Fuels 2025, 39, 9121−9133

current objective. Consequently, this study focuses on the experimental development of a catalytic packed bed reactor to analyze the effect of catalyst quantity on the catalytic hydrogen combustion process.

2. EXPERIMENTS

2.1. Experimental Setup and Equipment. The experimental setup, illustrated in Figure 2, consists of a regulated inflow system with a

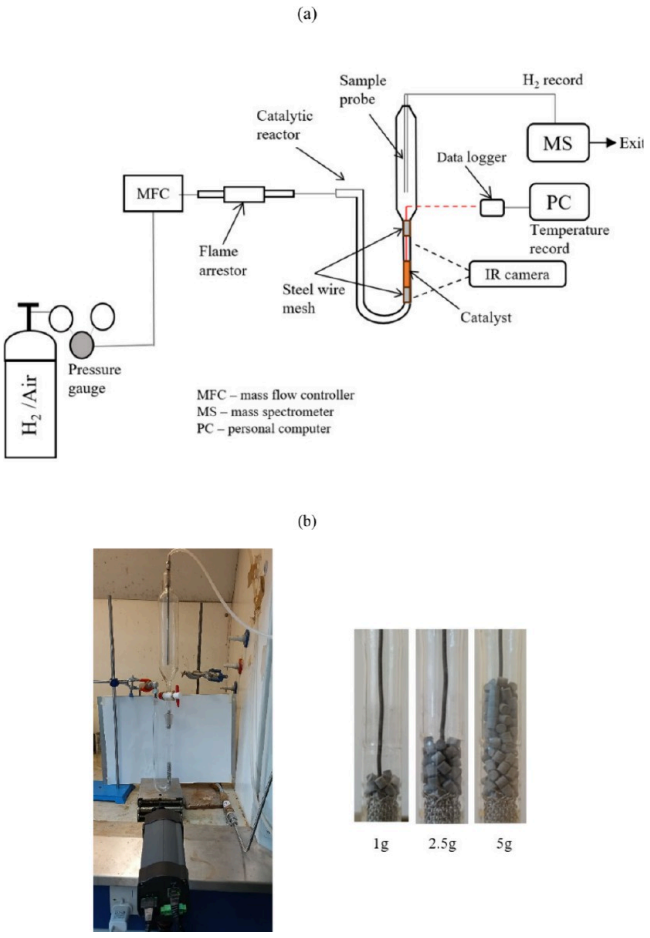

Figure 2. (a) Schematic view of the experimental setup. (b) Photograph of the experimental setup and catalyst loadings tested.

flame arrestor, a U-tube quartz reactor containing the packed bed of catalyst-coated alumina pellets, a diffuser glass tube attached to the reactor's exit to reduce flow velocity and aid in sample acquisition for the mass spectrometer, and a suite of detection instruments for measurement. The tube quartz reactor is 13 mm in diameter and 1 mm in thickness and is connected to inlet steel tubing. A hydrogen/air mixture (2% H_2 by volume) is supplied from a premixed cylinder. The gravitational stratification of mixture components is negligible here because only a fractional percentage variation is reported over a vertical distance of 15−20 m.[47] A mass flow controller (Alicat, MCP-100 SLPM-D/5M, 1% accuracy) is used to regulate the flow at 1 atm into the quartz reactor. Catalyst pellets are loaded inside the quartz reactor and placed at a particular position supported by a steel wire mesh. Another steel wire mesh is placed at the reactor exit for uniform flow of the combustion product. A gas sample probe is positioned at the center of the diffuser glass, from which the gas sample is drawn into a mass spectrometer to measure the concentration of H_2. The temperature of the catalyst is measured using an N-type thermocouple. The thermocouple probe tip is placed at the center location of the tube reactor and positioned while measuring the temperature at the bottom, middle, and top of the catalyst-packed bed. Moreover, an IR camera (FLIR A320, 320 × 240 pixels) is placed at a distance of 250 mm from the reactor front surface to capture the temperature distribution on the quartz tube wall.

2.2. Instrumentation. *2.2.1. Temperature Measurement.* An N-type thermocouple is used to measure the temperature of the catalytic bed, positioned at the desired location. The thermocouple's output is recorded using a Picolog-TC08 temperature data logger and stored on a computer hard drive.

Since the hydrogen combustion process is colorless, an infrared thermal camera is used to monitor and visualize the temperature distribution on the quartz wall of the reactor. The IR camera lens is positioned at a distance of 250 mm from the reactor front surface.

2.2.2. Mass Spectrometry (MS). Hydrogen gas detection is carried out using a quadrupole mass spectrometer (QMS; European Spectrometry Systems Ltd. GeneSys Evolution QMS400). The QMS consists of four key components. The ionizer bombards the gas sample with electrons to ionize the molecules. The ion accelerator propels these ions forward. The mass filter, composed of four parallel metal rods, selectively filters ions based on their mass-to-charge (m/z) ratio. Finally, the detector collects the filtered ions to ensure precise gas analysis. Only ions with a specific m/z ratio and corresponding to a given voltage ratio reach the detector, while ions with unstable trajectories are deflected and expelled after colliding with the rods. When an ion hits the detector, it generates an electrical current proportional to its abundance. These data are then processed by a computer to analyze the electrical current corresponding to the m/z ratios of the gas sample species.

2.2.3. Data Collection and Processing. The electrical current for gas species in the QMS is obtained using the multiple ion detection (MID) mode. In MID mode, gas species such as N_2, O_2, CO, Ar, and H_2 are detected by measuring the electrical current corresponding to their respective m/z ratios. Since the fuel mixture in the current analysis consists of 2% H_2 in air, and there is no significant change in the air composition after the catalytic process, only the H_2 concentration is calculated to assess performance.

To ensure accuracy, a background subtraction is performed in MID mode. For this, the inlet of the QMS is closed to create a zero-gas condition, which allows for subtraction of the background signals. This step is essential for detecting low concentrations of species, particularly H_2 in this case. Following background subtraction, the MID mode is calibrated using 2% H_2 in an air mixture at 1 bar. The sensitivity of the QMS to H_2 (K_{H_2}) for the m/z = 2.0 signal is then calculated using the following equation:

$$K_{H_2} = I_{H_2,\mathrm{ref}}/C_{H_2,\mathrm{ref}} \tag{3}$$

where

$$I_{H_2,\mathrm{ref}} = I_{H_2,\mathrm{total}} - I_{H_2,\mathrm{res}} \tag{4}$$

where $I_{H_2,\mathrm{ref}}$ is the reference current generated at the reference hydrogen concentration $C_{H_2,\mathrm{ref}}$, calculated by subtracting the residual current under zero-gas conditions from the total current. The hydrogen concentration under a particular operating condition (x) during the catalytic combustion process can be determined using the following equation:

$$C_{H_2}(x) = I_{H_2}(x)/K_{H_2} \tag{5}$$

where

$$I_{H_2}(x) = I_{H_2,\mathrm{total}}(x) - I_{H_2,\mathrm{res}}(x) \tag{6}$$

3. RESULTS AND DISCUSSION

To assess the catalytic performance, the flow rate of the premixed hydrogen/air (2% H_2) mixture through the catalytic packed bed reactor is varied to 1, 2, 3, 4, and 5 LPM at atmospheric pressure. The catalyst loadings in the catalyst bed are set at 1.0, 2.5, and 5.0 g. Two types of catalyst pellets (Pt/Al_2O_3 and Pd/Al_2O_3) are tested. The pellet sizes are 3 ± 0.2 mm.

https://doi.org/10.1021/acs.energyfuels.5c00576
Energy Fuels 2025, 39, 9121−9133

The characteristics of pellets at various catalyst contents are detailed in Table 1. The gas hourly space velocity (GHSV) and residence time for catalyst loadings tested are estimated for flow rates of 1, 2, 3, 4, and 5 LPM, as shown in Table 2. For catalyst bed weights of 1.0 and 2.5 g, the GHSV values are 5 times and 2 times that of the 5.0 g bed, respectively.

Table 1. List of Catalyst Samples

Catalyst type	Supplier	Av pore radius (Å)	BET specific surface area (m^2/g)	Total pore vol (cc/g)
0.3% Pt/Al_2O_3	Thermo Scientific	47.3	118.22	0.279
0.5% Pt/Al_2O_3	Johnson Matthey	53.3	92.716	0.247
1.0% Pt/Al_2O_3	Thermo Scientific	52.2	96.742	0.252
0.5% Pd/Al_2O_3	Alfa Aesar	46.7	112.261	0.262
5.0% Pd/Al_2O_3	Thermo Scientific	50.7	224.255	0.568

3.1. Reactor Temperatures. Figures 3−6 present reactor wall temperature maps of the listed sample in Table 1 for various flow rates and catalyst loadings. Although the temperatures shown do not represent the exact inner wall temperatures due to emissivity losses in the quartz wall, the thermal images captured by the IR camera still provide valuable insights into the internal catalytic processes and heat transfer dynamics of the reacting flow.

In Figure 3a, for the 0.5% Pt/Al_2O_3 catalyst with a 1.0 g loading, the wall temperatures at the catalyst location range from 55 to 60 °C and remain relatively constant across all flow rates. However, as the flow rate increases, the heated region of the wall expands, indicating an enhanced convective heat transfer. When the catalyst loading increases to 2.5 g, as shown in Figure 3b, the wall temperatures rise significantly, with peak values ranging between 80 and 100 °C. As expected, both the extent of the heated region and the wall temperatures increase with higher flow rates. Further increasing the catalyst loading to 5.0 g does not result in higher maximum wall temperatures compared to the 2.5 g case, but the heated region continues to expand with an increasing flow rate. The larger heated area at higher catalyst loadings is attributed to the increased thermal mass of the additional catalyst.

For the 1.0% Pt/Al_2O_3 catalyst, as depicted in Figure 4, the wall temperatures are captured under the same inflow conditions and catalyst loadings as those of 0.5% Pt/Al_2O_3 catalyst. The heated region at the catalyst location, along with the pattern of expanding heated areas with higher flow rates, is very similar to that of the 0.5% Pt/Al_2O_3 case. However, the wall temperatures for the 1.0% Pt/Al_2O_3 catalyst are consistently higher across all of the studied conditions, indicating greater heat generation from the catalytic process. The increased catalytic activity of the 1.0% Pt/Al_2O_3 catalyst can be attributed to its higher platinum content. To further investigate the effect of catalyst content, 0.3% Pt/Al_2O_3 catalyst of similar characteristics as mentioned in Table 1 is tested under the same operating conditions as 0.5% Pt/Al_2O_3 and 1.0% $Pt/Pt/Al_2O_3$. Interestingly, no catalytic activity is observed with the 0.3% Pt/Al_2O_3 catalyst, likely due to its low platinum content.

Similarly, the wall temperature maps for 0.5%Pd/Al_2O_3 and 5%Pd/Al_2O_3 catalysts are presented at different catalyst loadings in Figure 5 and Figure 6. The results show that these catalysts are also effective for hydrogen oxidation and producing heat. However, the relative effect of catalysts on the catalytic combustion process and catalyst temperatures is discussed in the following section.

To gain better understanding of the catalyst temperatures during the catalytic combustion process, a thermocouple is used and positioned for measuring temperatures at the bottom, middle, and top locations of the catalytic packed bed. As expected, measured catalyst temperatures are significantly higher than the wall temperatures. Figure 7 and Figure 8 present the temperature profiles as functions of flow rates for the 0.5% Pt/Al_2O_3 and 1.0% Pt/Al_2O_3 catalysts, respectively. The vertical bar in both plots presents the measurement uncertainty. For the 0.5% Pt/Al_2O_3 catalyst with a 1 g loading, the temperature at the bottom of the bed decreases with increasing flow rates, while the temperature at the middle remains consistently high, around 140 °C, across all flow rates. At the top of the bed, temperatures are about 15 °C lower than at the middle but increase slightly with flow rate due to enhanced convective heat transfer. When the catalyst loading is increased to 2.5 g, the temperature at the bottom reaches a maximum at 2 LPM before decreasing with higher flow rates. The temperatures at the middle and top of the bed increase with flow rate, with a temperature difference of approximately 20 °C between the two locations. Overall, the temperature values for the 2.5 g catalyst loading are higher than those for the 1 g loading due to the increased catalyst mass involved in the catalytic process. For the 5.0 g catalyst loading, the bottom location temperatures are higher than those for the 2.5 g case but follow a similar trend with flow rates.

The temperatures at the middle remain in a similar range as for the 2.5 g loading, while the top temperatures are comparatively lower, likely due to the thicker catalytic bed, which hinders heat dissipation with increased flow rates. For the 1.0% Pt/Al_2O_3 catalyst, as shown in Figure 8, the temperature profiles under similar inflow and catalyst loading conditions are like the 0.5% Pt/Al_2O_3 catalyst. However, the overall temperatures are higher, indicating increased heat generation from the catalytic process due to the higher platinum content. Unlike the 0.5% Pt/Al_2O_3 catalyst, the maximum temperatures at the bottom of the bed for the 1.0% Pt/Al_2O_3 catalyst are observed for both the 2.5 and 5.0 g loadings. Interestingly, in both cases, the temperatures are experienced above the adiabatic temper-

Table 2. GHSV and Residence Time for the Catalysts

	GHSV (h^{-1})			Residence time (s)		
LPM	1 g	2.5 g	5 g	1 g	2.5 g	5 g
1	237600	95040	47520	0.01515	0.03787	0.07575
2	475200	190080	95040	0.00757	0.01893	0.03787
3	712800	285120	142560	0.00505	0.01262	0.02525
4	950400	380160	190080	0.00378	0.00946	0.01893
5	1188000	475200	237600	0.00303	0.00757	0.01515

https://doi.org/10.1021/acs.energyfuels.5c00576
Energy Fuels 2025, 39, 9121−9133

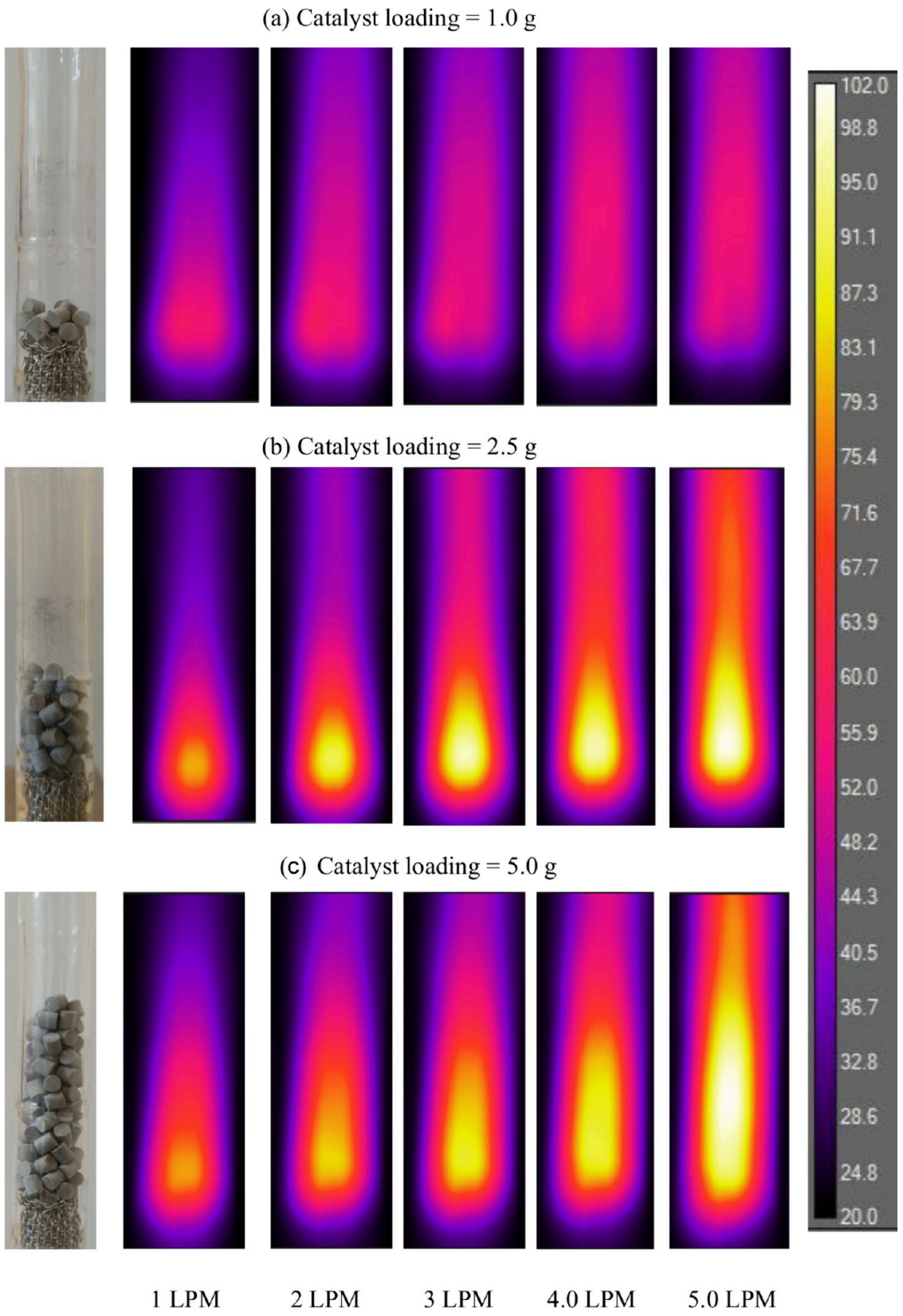

Figure 3. Reactor wall temperatures (°C) obtained from IR thermal camera, 0.5% Pt/Al_2O_3.

atures (~178 °C). Furthermore, in both cases, the observed temperatures exceed the adiabatic limit (~178 °C) at the front location of the catalyst bed, highlighting the superadiabatic nature of the catalytic process, which is attributed to the low Lewis number of the hydrogen/air mixture.[9,48,49]

Additionally, the temperatures at the middle and top of the bed increase with flow rates, with temperature differences

https://doi.org/10.1021/acs.energyfuels.5c00576
Energy Fuels 2025, 39, 9121−9133

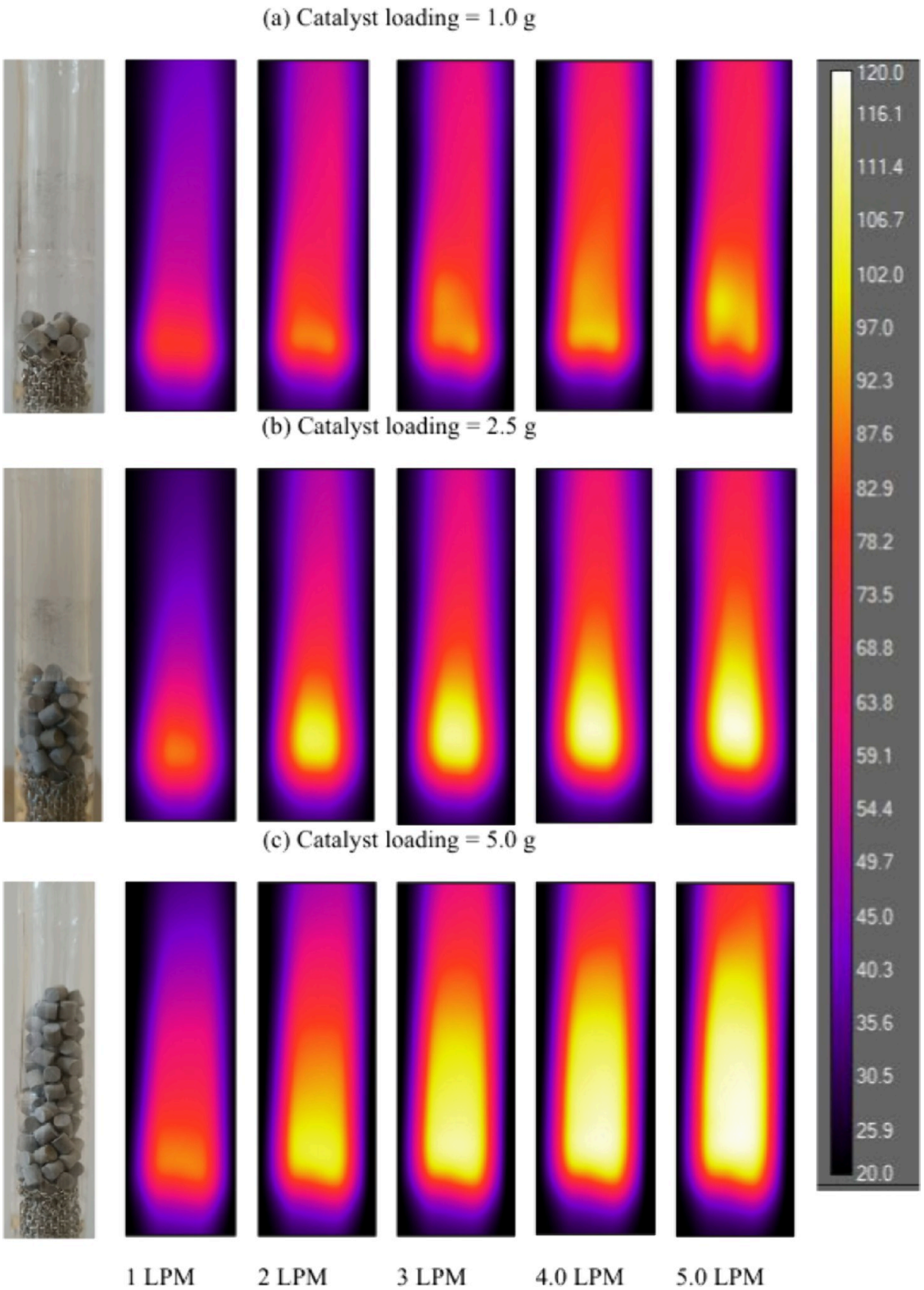

Figure 4. Reactor wall temperatures (°C) obtained from IR thermal camera, 1.0% Pt/Al_2O_3.

between the locations of approximately 20 and 40 °C for 2.5 and 5.0 g loadings, respectively. Similarly, the profiles of catalyst bed temperatures for 0.5% Pd/Al_2O_3 and 5.0% Pd/Al_2O_3 at different locations are illustrated in Figure 9 and Figure 10, respectively. The trend of the profiles with flow rate is similar to that experienced for 0.5% Pt/Al_2O_3 and 1.0% Pt/Al_2O_3 in Figure 7 and Figure 8. In addition, superadiabatic temperatures are observed for 5.0% Pd/Al_2O_3 catalysts at the front location of the catalyst bed, while operating at higher flow rates. Because the temperatures exceed the adiabatic flame temperature (∼178 °C), this phenomenon occurs due to the diffusional imbalance of the H_2/air mixture, as the Lewis number (Le) for hydrogen is below unity ($Le = 0.3$). Consequently, hydrogen's strong affinity for the hot reaction zone results in a relatively rich mixture and

https://doi.org/10.1021/acs.energyfuels.5c00576
Energy Fuels 2025, 39, 9121−9133

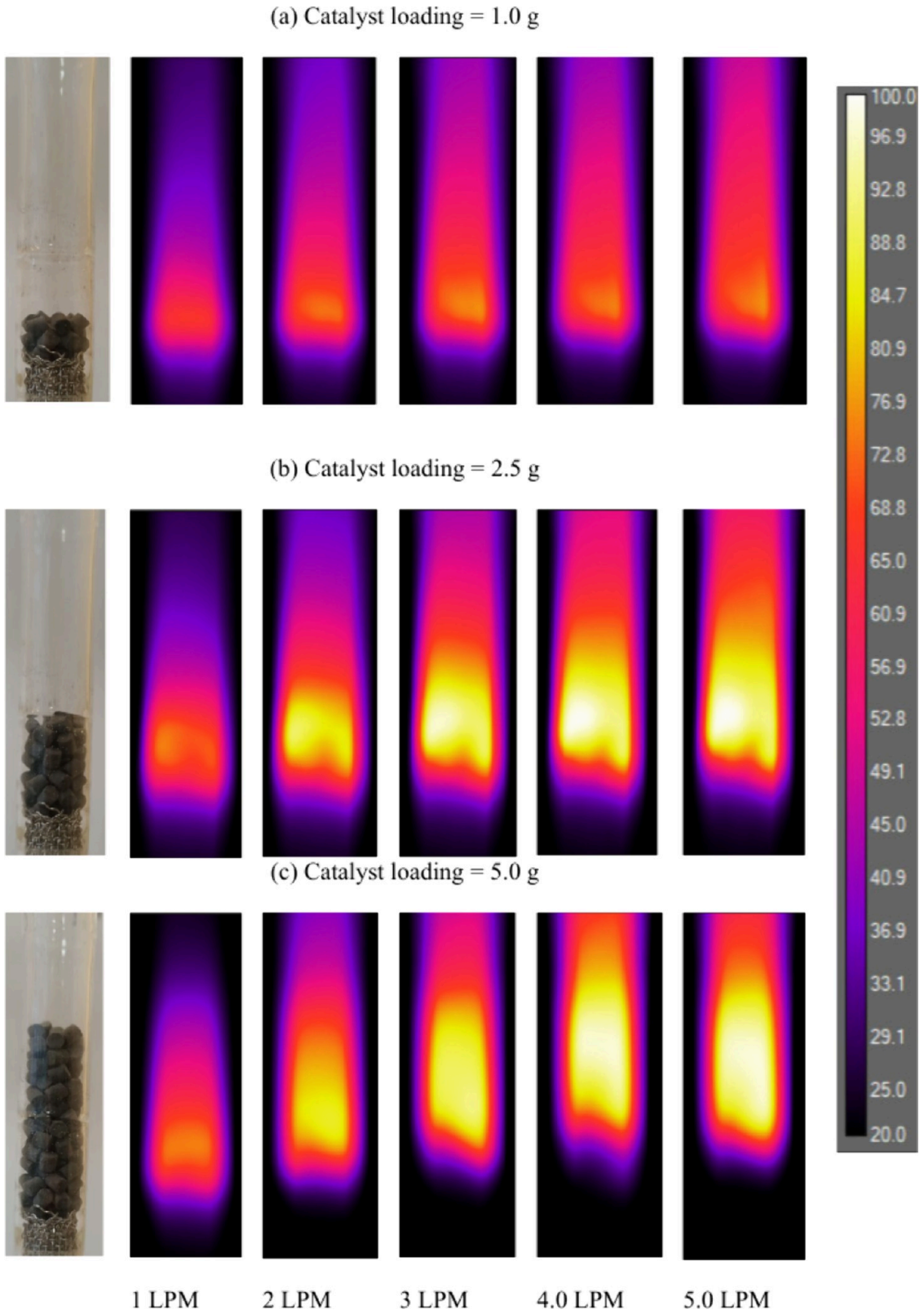

Figure 5. Reactor wall temperatures (°C) obtained from IR thermal camera, 0.5% Pd/Al_2O_3.

elevated temperatures.[31,39] This indicates that high catalyst content enhances the catalytic process and leads to a superadiabatic temperature. However, to have a better understanding of the catalytic process, the effect of the catalyst content and various catalyst loadings on the catalytic conversion rates is discussed in the following section.

3.2. H_2 Conversions. Hydrogen (H_2) conversions for the studied cases are shown in Figure 11 for the 0.5% Pt/Al_2O_3 and 1.0% Pt/Al_2O_3 catalysts, respectively. The vertical bar is used in both plots to present the measurement uncertainty. In all cases, H_2 conversion is highest at low flow rates due to the increased residence time and decreases as flow rates increase. For the 0.5%

https://doi.org/10.1021/acs.energyfuels.5c00576
Energy Fuels 2025, 39, 9121−9133

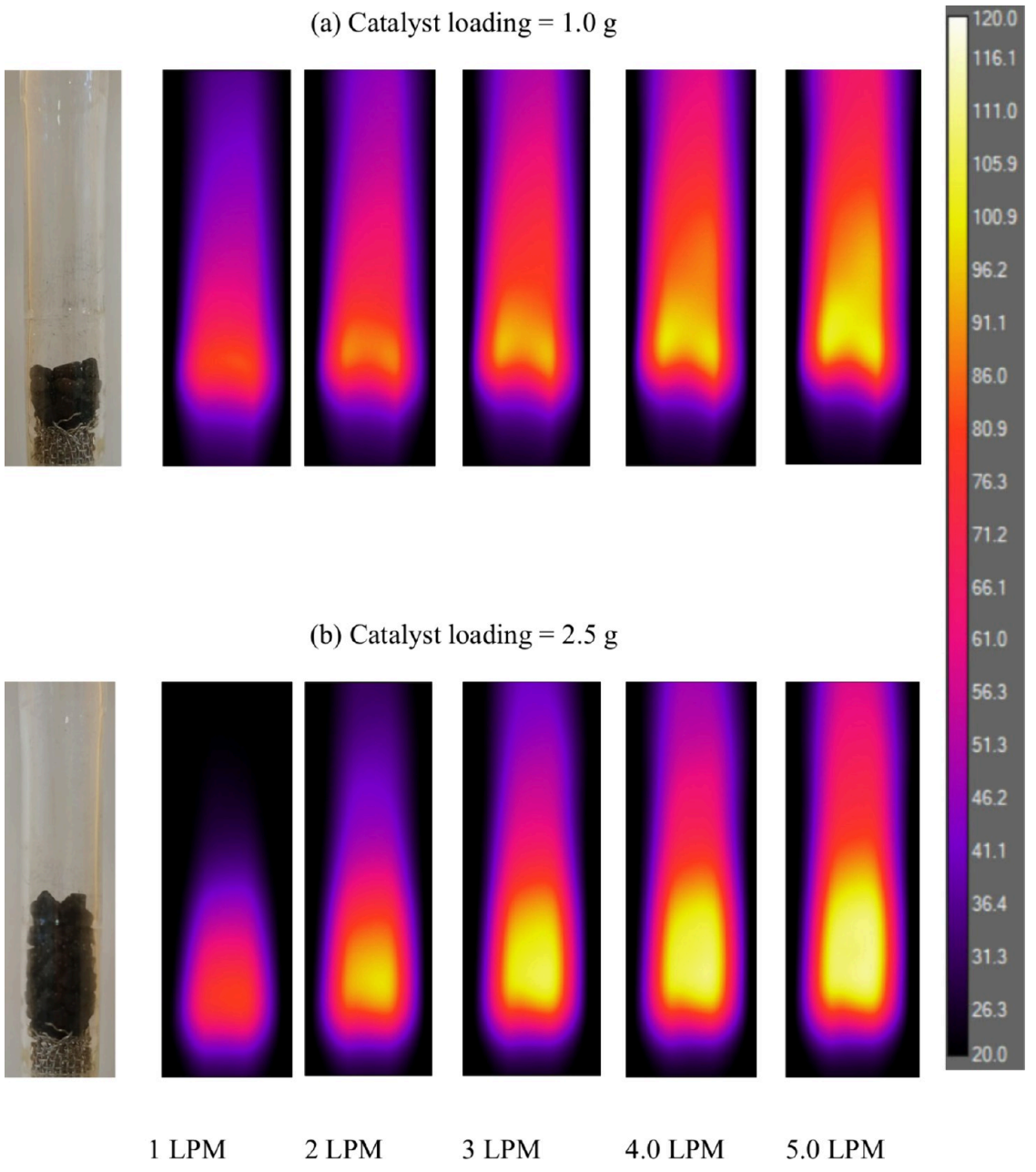

Figure 6. Reactor wall temperatures (°C) obtained from IR thermal camera, 5.0% Pd/Al_2O_3.

Pt/Al_2O_3 catalyst at a 1 g loading, H_2 conversions are significantly lower compared to those of the 1.0% Pt/Al_2O_3 catalyst, indicating that the higher platinum content in the 1.0% Pt/Al_2O_3 catalyst has a considerable impact on the catalytic process.

Interestingly, the H_2 conversions for the 0.5% Pt/Al_2O_3 catalyst at 2.5 and 5.0 g loadings are nearly comparable to the conversion values at 1.0 and 2.5 g loadings of the 1.0% Pt/Al_2O_3 catalyst, further emphasizing the effect of platinum content on catalytic performance. At a 5 g loading of the 1.0% Pt/Al_2O_3 catalyst, H_2 conversions reach nearly 100% across all flow rates, demonstrating enhanced catalytic efficiency due to the higher platinum content.

Similarly, Figure 12 presents the H_2 conversion rates for the Pd/Al_2O_3 catalysts at various catalyst loadings and flow rates. As previously discussed, catalyst content plays a crucial role in the catalytic process. Accordingly, the H_2 conversion achieved with 5% Pd/Al_2O_3 is significantly higher than that with 0.5% Pd/Al_2O_3 at the same catalyst loading. Notably, for a catalyst loading of 2.5 g in 5% Pd/Al_2O_3, nearly 100% conversion is observed across all flow rates. However, it is quite convincing that the conversion will be 100% if the catalyst loading is increased; therefore, the catalyst loading of 5 g for in 5% Pd/Al_2O_3 is not tested.

3.3. Catalytic Reaction Mechanism. It is generally agreed that the reaction mechanism is of a Langmuir−Hinshelwood type with both reactants dissociating on the platinum surface.[50,51] Although it is a seemingly simple reaction, there is not a single agreed mechanism. Nevertheless, all mechanisms have one of the following steps as a key to the formation of water.

$$OH_{(ads)} + OH_{(ads)} \rightarrow H_2O_{(ads)} + O_{(ads)} \quad (7)$$

$$H_{(ads)} + OH_{(ads)} \rightarrow H_2O_{(ads)} \quad (8)$$

https://doi.org/10.1021/acs.energyfuels.5c00576
Energy Fuels 2025, 39, 9121−9133

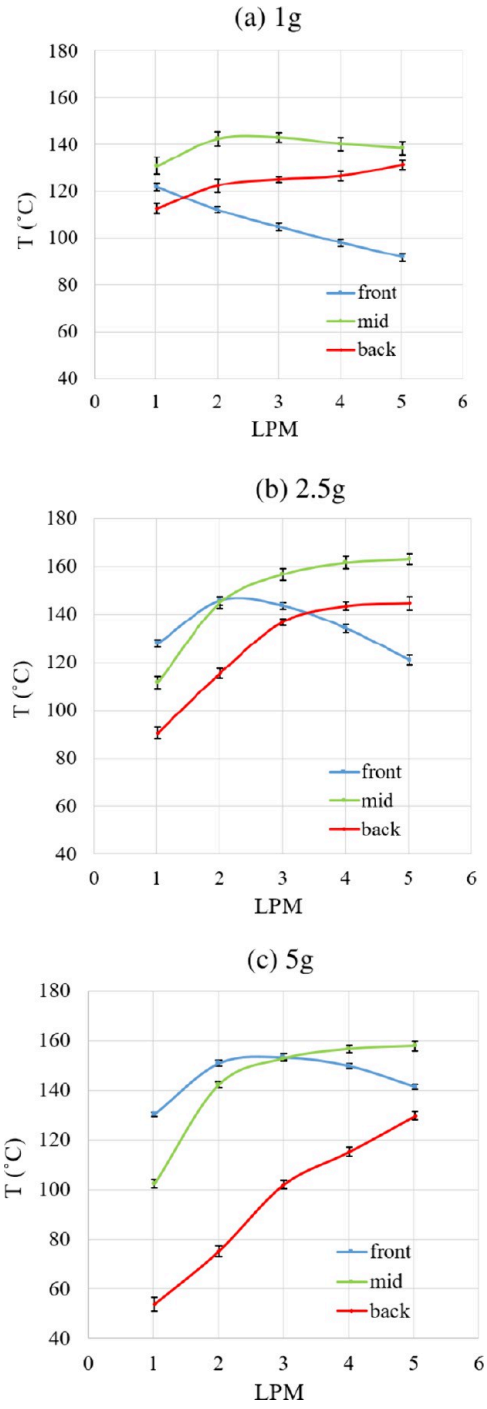

Figure 7. Catalyst (0.5% Pt/Al_2O_3) bed temperatures at different locations for loading: (a) 1, (b) 2.5, and (c) 5 g.

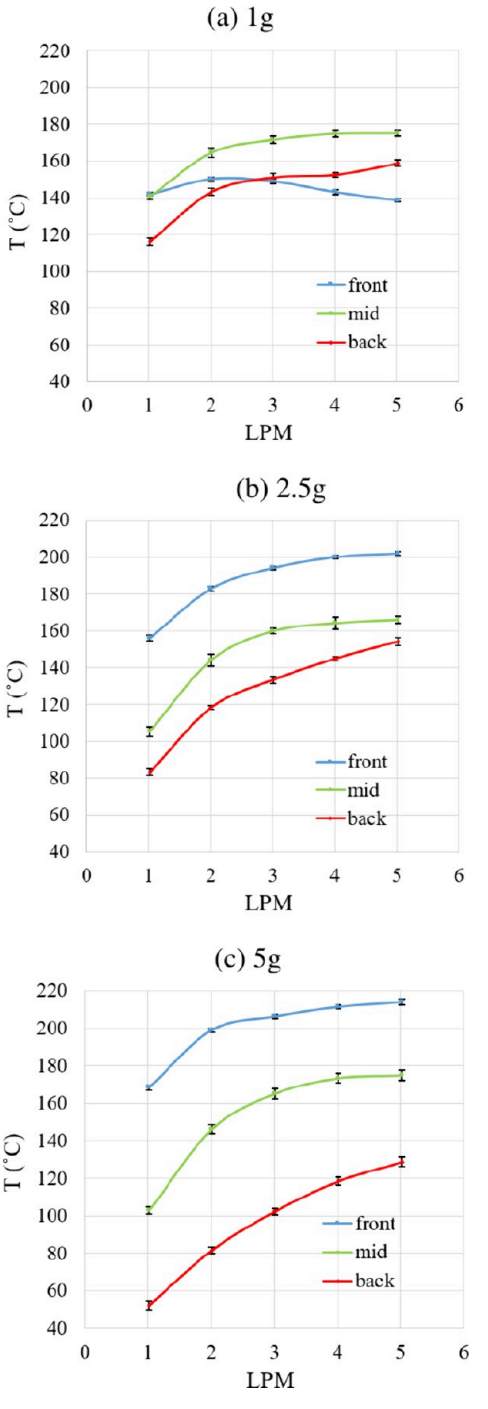

Figure 8. Catalyst (1% Pt/Al_2O_3) bed temperatures at different locations for loading: (a) 1, (b) 2.5, and (c) 5 g.

It has been suggested that the first equation may go through a short-lived H_2O_2 peroxide species,

$$OH_{(ads)} + OH_{(ads)} \rightarrow H_2O_{2(ads)} \rightarrow H_2O_{(ads)} + O_{(ads)} \quad (9)$$

As discussed, the catalytic loadings significantly affect the catalytic H_2 conversion and combustion temperatures. These effects can be described using the apparent kinetic parameters, such as the reaction rate constant (k) and activation energy (E_a). The values of k and E_a for different catalyst loadings in Table 3 and Table 4 are estimated by using H_2 conversion, residence time, and average catalyst bed temperatures. The increase in catalyst loading has two effects: first, a more active phase is available; second, the residence time increases, allowing more time for conversion. When using loadings of 2.5 and 5 g for a particular flow rate, there are 2.5 and 5 times more active sites available compared to a 1 g loading. As a result, the process is controlled by combustion diffusion and the rate constant decreases with increased loading for all catalysts, as shown in Table 3. As the flow rate increases for a particular catalyst loading, the quantity of hydrogen passing over the catalyst and engaging in reactions also rises. Consequently, at 5 LPM, five times more hydrogen reacts compared to 1 LPM. In this scenario, the catalytic process is kinetically controlled, which

https://doi.org/10.1021/acs.energyfuels.5c00576
Energy Fuels 2025, 39, 9121−9133

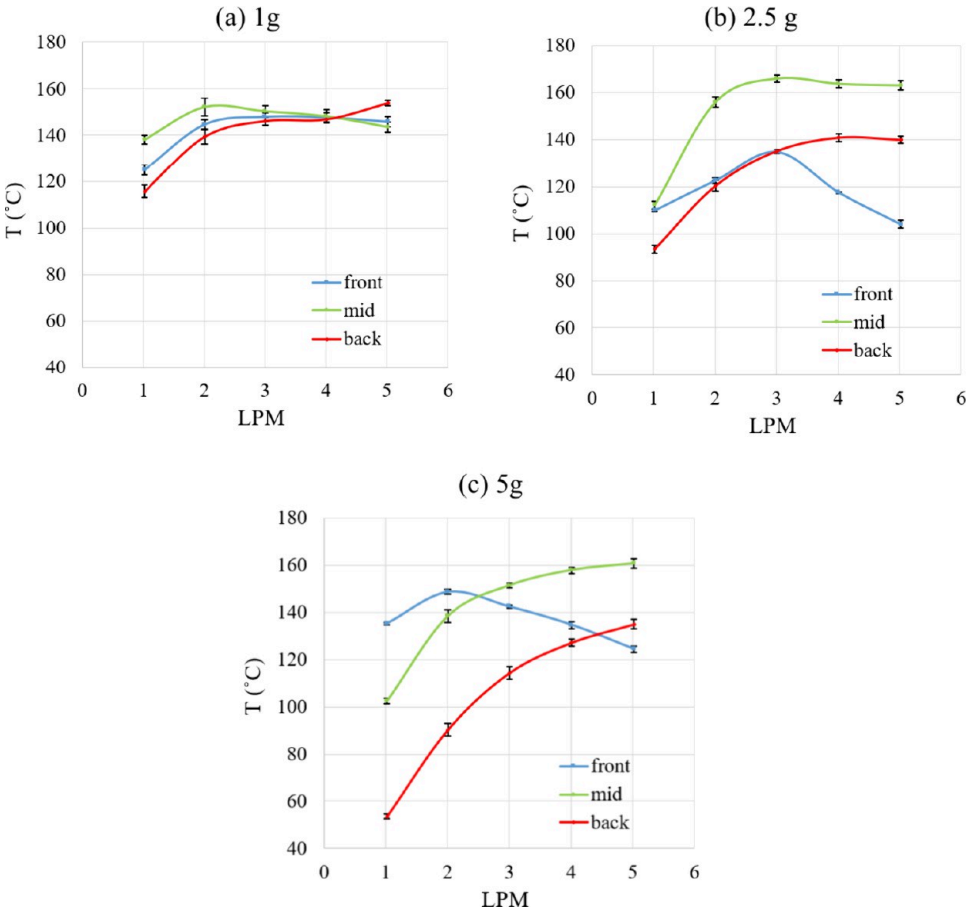

Figure 9. Catalyst (0.5% Pd/Al_2O_3) bed temperatures at different locations for loading: (a) 1, (b) 2.5, and (c) 5 g.

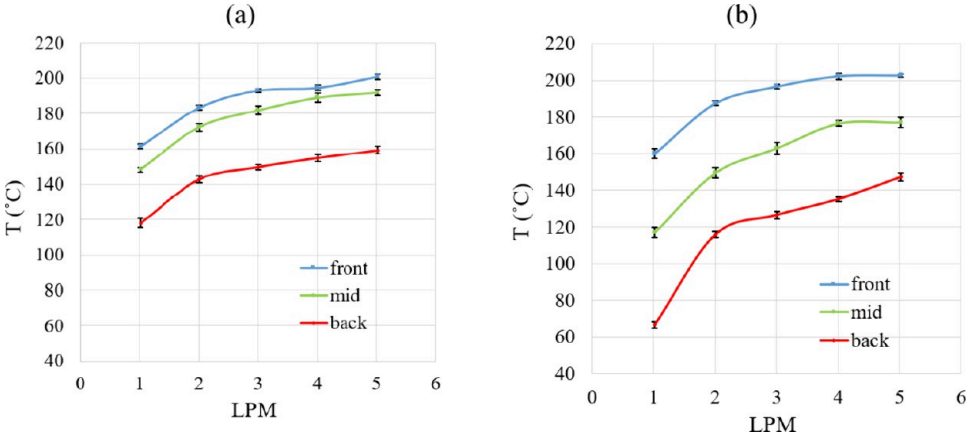

Figure 10. Catalyst (5% Pd/Al_2O_3) bed temperatures at different locations for loading: (a) 1 and (b) 2.5 g.

means that the rate constant values increase with LPM across all catalyst loadings. The apparent activation energies in Table 4 also reflect how catalyst loading influences the reaction mechanism. At a low catalyst loading, the process is primarily controlled by kinetics and has higher E_a values. As the loading increases, the process shifts to a diffusion-dominated regime, leading to a decrease in the E_a values.

However, the number of reaction cycles significantly influences the catalytic performance and long-term stability of a catalyst, which can lead to catalyst deactivation.[52] Typically in this reaction, deactivation is highly sensitive to reaction temperature. This reflects that the main cause of deactivation is likely to be sintering. The interconversion of the platinum crystallite between oxidized and reduced forms and the presence of steam are all contributing factors to sintering not just of the platinum but of the support material.[5] Hence pretreatment of the catalyst at temperatures above the reaction temperature would be expected to enhance catalyst lifetimes and some studies[53−55] have indicated that catalysts calcined at high temperatures and Al anodization exhibit increased durability. Water can also have a role in catalyst deactivation; as the concentration increases, the potential for capillary condensation in small pores of the support increases with the potential for blocking off platinum crystallites within the pores. This behavior

https://doi.org/10.1021/acs.energyfuels.5c00576
Energy Fuels 2025, 39, 9121−9133

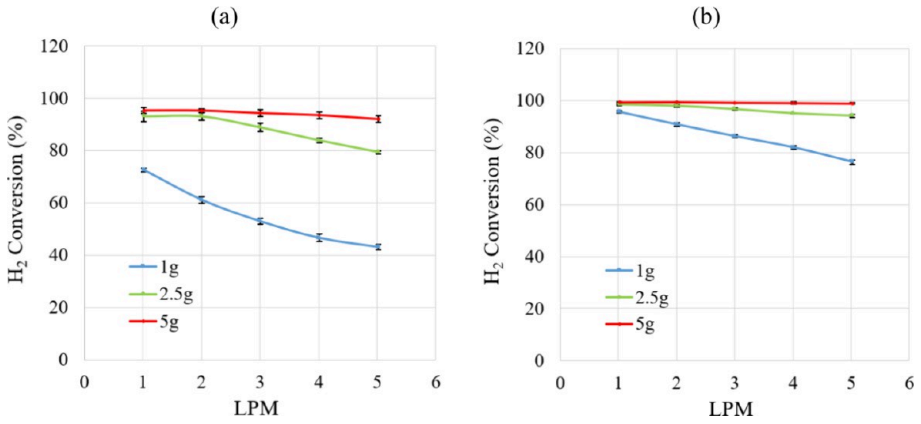

Figure 11. Effect of catalyst loading on hydrogen conversion for (a) 0.5% Pt/Al_2O_3 and (b) 1% Pt/Al_2O_3.

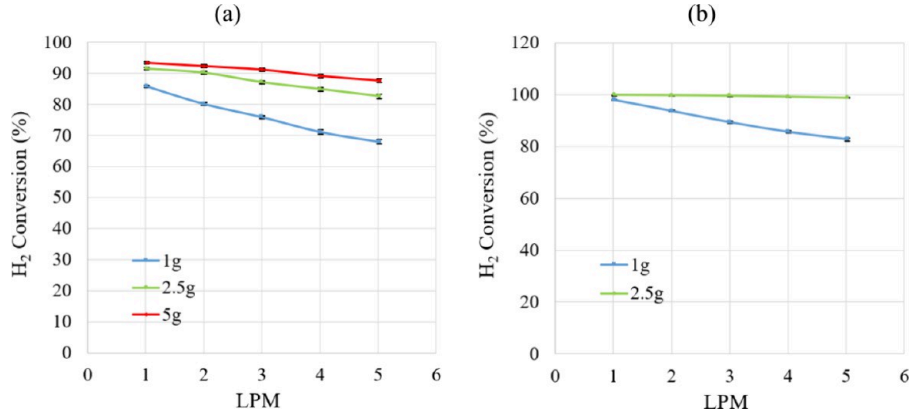

Figure 12. Effect of catalyst loading on hydrogen conversion for (a) 0.5% Pd/Al_2O_3 and (b) 5% Pd/Al_2O_3.

Table 3. Reaction Rate Constant, k (s^{-1})

	0.5%Pt/Al_2O_3			1%%Pt/Al_2O_3			0.5%Pd/Al_2O_3			5%Pd/Al_2O_3	
LPM	1 g	2.5 g	5 g	1 g	2.5 g	5 g	1 g	2.5 g	5 g	1 g	2.5 g
1.0	47.8	24.6	12.6	63.1	25.9	13.1	56.5	24.1	12.3	64.7	26.3
2.0	80.6	49.1	25.1	119.9	51.6	26.2	105.6	47.6	24.4	123.8	52.6
3.0	104.9	70.3	37.3	170.8	76.4	39.3	150.1	69.0	36.1	177.0	78.8
4.0	123.0	88.5	49.3	216.3	100.7	52.3	187.5	89.6	47.0	225.9	104.9
5.0	142.3	104.7	60.7	252.0	124.3	65.2	224.1	109.0	57.8	272.9	130.4

Table 4. Activation Energy, E_a (kJ/mol)

Catalyst loading	1 g	2.5 g	5 g
0.5%Pt/Al_2O_3	68.803	47.107	39.642
1%%Pt/Al_2O_3	56.626	36.673	33.688
0.5%Pd/Al_2O_3	72.872	49.075	41.215
5%Pd/Al_2O_3	53.775	36.241	

can be expected at high partial pressures of water coupled to low reactor temperatures and would worsen with time on stream.

4. CONCLUSIONS

Experiments on the catalytic combustion of ultra-lean hydrogen/air mixtures (2% H_2 by volume) were conducted in a catalytic packed-bed tubular reactor to assess the impact of catalyst loading on the catalytic process. The key findings from the experimental results are summarized as follows:

- The temperatures at the middle and top locations of the catalyst packed bed increase with rising flow rates for both the Pt/Al_2O_3 and Pd/Al_2O_3 catalysts.
- Superadiabatic temperatures are observed at the bottom location for the 1% Pt/Al_2O_3 catalyst with 2.5 and 5 g loadings and for the 5% Pd/Al_2O_3 catalyst with 1.0 and 2.5 g loadings.
- For the same catalyst loading with high catalyst content, the overall temperatures are higher compared to the low catalyst content.
- In all cases, H_2 conversion is highest at low flow rates due to the increased residence time, which favors the catalytic process.
- For the same catalyst loading, H_2 conversions are significantly higher for the 1% Pt/Al_2O_3 catalyst than for the 0.5% Pt/Al_2O_3 catalyst, owing to the higher platinum content in the 1% Pt/Al_2O_3 catalyst, facilitating the catalytic process. Due to the same reason, the H_2 conversions for 5% Pd/Al_2O_3 are observed higher than 0.5% Pd/Al_2O_3.

https://doi.org/10.1021/acs.energyfuels.5c00576
Energy Fuels 2025, 39, 9121−9133

- In high content catalyst, the catalytic performance at a low flow rate with a catalyst loading of 1 g is comparable to that observed under other catalyst loadings and flow conditions.
- At low catalyst loading, the catalytic process is controlled by kinetics, while increasing catalyst loading shifts the process to diffusion control.

■ ASSOCIATED CONTENT

Data Availability Statement

Data will be made available on request.

■ AUTHOR INFORMATION

Corresponding Author

Manosh C. Paul − *James Watt School of Engineering, University of Glasgow, Glasgow G12 8QQ, United Kingdom;* orcid.org/0000-0002-6510-456X; Email: Manosh.Paul@glasgow.ac.uk

Authors

Md Nur Alam Mondal − *James Watt School of Engineering, University of Glasgow, Glasgow G12 8QQ, United Kingdom; Department of Mechanical Engineering, Hajee Mohammad Danesh Science and Technology University, Dinajpur 5200, Bangladesh*

Nader Karimi − *James Watt School of Engineering, University of Glasgow, Glasgow G12 8QQ, United Kingdom; School of Engineering and Materials Science, Queen Mary University of London, London E14 NS, United Kingdom;* orcid.org/0000-0002-4559-6245

S. David Jackson − *School of Chemistry, University of Glasgow, Glasgow G12 8QQ, United Kingdom;* orcid.org/0000-0003-1257-5533

Complete contact information is available at: https://pubs.acs.org/10.1021/acs.energyfuels.5c00576

Notes

The authors declare no competing financial interest.

■ ACKNOWLEDGMENTS

M.N.A.M. is a Commonwealth Scholar (CSC ID: BDCS-2020-54), funded by the U.K. government. We acknowledge the help of Dr. Emma Gibbson and Ahmed Mohamed Radwan in the experiments and the support from the School of Chemistry at the University of Glasgow.

■ REFERENCES

(1) Zhou, H.; Xue, J.; Gao, H.; Ma, N. Hydrogen-fueled gas turbines in future energy system. *Int. J. Hydrogen Energy* **2024**, *64*, 569−582.

(2) Boretti, A. Towards hydrogen gas turbine engines aviation: A review of production, infrastructure, storage, aircraft design and combustion technologies. *Int. J. Hydrogen Energy* **2024**, *88*, 279−288.

(3) Wang, S.; Chen, L.; Niu, F.; Chen, D.; Qin, L.; Sun, X.; Huang, Y. Catalytic combustion of hydrogen for residential heat supply application. *Int. J. Energy Res.* **2016**, *40*, 1979−1985.

(4) Pan, J.; Miao, N.; Lu, Z.; Lu, Q.; Yang, W.; Pan, Z.; Zhang, Y. Experimental and numerical study on the transition conditions and influencing factors of hetero-/homogeneous reaction for H2/Air mixture in micro catalytic combustor. *Appl. Therm Eng.* **2019**, *154*, 120−130.

(5) Kim, J.; Yu, J.; Lee, S.; Tahmasebi, A.; Jeon, C.-H.; Lucas, J. Advances in catalytic hydrogen combustion research: Catalysts, mechanism, kinetics, and reactor designs. *Int. J. Hydrogen Energy* **2021**, *46*, 40073−40104.

(6) He, L.; Fan, Y.; Bellettre, J.; Yue, J.; Luo, L. A review on catalytic methane combustion at low temperatures: Catalysts, mechanisms, reaction conditions and reactor designs. *Renewable and Sustainable Energy Reviews* **2020**, *119*, No. 109589.

(7) Ibrahim, H. A.; Ahmed, W. H.; Abdou, S.; Blagojevic, V. Experimental and numerical investigations of flow through catalytic converters. *Int. J. Heat Mass Transf* **2018**, *127*, 546−560.

(8) Sui, R.; Prasianakis, N. I.; Mantzaras, J.; Mallya, N.; Theile, J.; Lagrange, D.; Friess, M. An experimental and numerical investigation of the combustion and heat transfer characteristics of hydrogen-fueled catalytic microreactors. *Chem. Eng. Sci.* **2016**, *141*, 214−230.

(9) Battistella, F.; Donazzi, A.; Ravidà, A.; Valenti, G.; Groppi, G. Numerical modeling and experimental testing of the hydrogen ultralean combustion on an adiabatic catalytic monolith in diverse working conditions. *Int. J. Hydrogen Energy* **2024**, *71*, 1405−1415.

(10) Zhou, H.; Xue, J.; Gao, H.; Ma, N. Hydrogen-fueled gas turbines in future energy system. *Int. J. Hydrogen Energy* **2024**, *64*, 569−582.

(11) Saint-Just, J.; Etemad, S. Catalytic combustion of hydrogen for heat production. In *Compendium of Hydrogen Energy*, Vol. 3; Elsevier, 2016: pp 263−287. DOI: 10.1016/B978-1-78242-363-8.00010-4.

(12) Guan, B.; Zhan, R.; Lin, H.; Huang, Z. Review of state of the art technologies of selective catalytic reduction of NOx from diesel engine exhaust. *Appl. Therm Eng.* **2014**, *66*, 395−414.

(13) Resitoglu, I. A.; Keskin, A. Hydrogen applications in selective catalytic reduction of NOx emissions from diesel engines. *Int. J. Hydrogen Energy* **2017**, *42*, 23389−23394.

(14) Roy, S.; Hegde, M. S.; Madras, G. Catalysis for NOx abatement. *Appl. Energy* **2009**, *86*, 2283−2297.

(15) Granger, P.; Dhainaut, F.; Pietrzik, S.; Malfoy, P.; Mamede, A. S.; Leclercq, L.; Leclercq, G. An overview: Comparative kinetic behaviour of Pt, Rh and Pd in the NO + CO and NO + H2 reactions. *Top Catal* **2006**, *39*, 65−76.

(16) Hayes, R. E.; Kolaczkowski, S. T. *Introduction to Catalytic Combustion*; Routledge: London, 2021. DOI: 10.1201/9780203750186.

(17) Yuan, L.-J.; Zhao, Z.-C.; Wang, W.-Q.; Wang, Y.-F.; Liu, Y.-J. Review of Catalysts, Substrates, and Fabrication Methods in Catalytic Hydrogen Combustion with Further Challenges and Applications. *Energy Fuels* **2024**, *38*, 4881−4903.

(18) HARUTA, M.; SANO, H. Catalytic combustion of hydrogen I—Its role in hydrogen utilization system and screening of catalyst materials. *Int. J. Hydrogen Energy* **1981**, *6*, 601−608.

(19) Buciuman, F.-C.; Patcas, F.; Menezo, J.-C.; Barbier, J.; Hahn, T.; Lintz, H.-G. Catalytic properties of La0.8A0.2MnO3 (A = Sr, Ba, K, Cs) and LaMn0.8B0.2O3 (B = Ni, Zn, Cu) perovskites1. Oxidation of hydrogen and propene. *Appl. Catal., B* **2002**, *35*, 175−183.

(20) Eom, H.-J.; Jang, J. H.; Lee, D.-W.; Kim, S.; Lee, K.-Y. Catalytic combustion of hydrogen over La1−xSrxCoO3−δ+Co3O4 and LaMn1−xCuxO3+δ under simulated MCFC anode off-gas conditions. *J. Mol. Catal. A Chem.* **2011**, *349*, 48−54.

(21) Pizza, G.; Frouzakis, C. E.; Mantzaras, J. Chaotic dynamics in premixed hydrogen/air channel flow combustion. *Combustion Theory and Modelling* **2012**, *16*, 275−299.

(22) Pers, H.; Aniello, A.; Morisseau, F.; Schuller, T. Autoignition-induced flashback in hydrogen-enriched laminar premixed burners. *Int. J. Hydrogen Energy* **2023**, *48*, 10235.

(23) Yang, Z.; Li, D.; Wang, L. Research on the hot surface ignition of hydrogen-air mixture under different influencing factors. *Int. J. Energy Res.* **2018**, *42*, 3966−3976.

(24) Day, M. S.; Bell, J. B.; Gao, X.; Glarborg, P. Numerical simulation of nitrogen oxide formation in lean premixed turbulent H2/O2/N2 flames. *Proceedings of the Combustion Institute* **2011**, *33*, 1591−1599.

(25) Yilmaz, H.; Cam, O.; Yilmaz, I. Effect of micro combustor geometry on combustion and emission behavior of premixed hydrogen/air flames. *Energy* **2017**, *135*, 585−597.

(26) Meraner, C.; Li, T.; Ditaranto, M.; Løvås, T. Combustion and NO_x Emission Characteristics of a Bluff Body Hydrogen Burner. *Energy Fuels* **2019**, *33*, 4598−4610.

(27) Resende, P.R.; Afonso, A.; Pinho, C.; Ayoobi, M. Impacts of Dilution on Hydrogen Combustion Characteristics and NOx Emissions. *J. Heat Transfer* **2019**, *141*, 012003.
(28) Boulahlib, M. S.; Medaerts, F.; Boukhalfa, M. A. Experimental study of a domestic boiler using hydrogen methane blend and fuel-rich staged combustion. *Int. J. Hydrogen Energy* **2021**, *46*, 37628−37640.
(29) ILBAS, M.; YILMAZ, I.; KAPLAN, Y. Investigations of hydrogen and hydrogen−hydrocarbon composite fuel combustion and emission characteristics in a model combustor. *Int. J. Hydrogen Energy* **2005**, *30*, 1139−1147.
(30) Fumey, B.; Buetler, T.; Vogt, U. F. Ultra-low NOx emissions from catalytic hydrogen combustion. *Appl. Energy* **2018**, *213*, 334−342.
(31) Mondal, M. N. A.; Karimi, N.; Jackson, S. D.; Paul, M. C. Numerical investigation of premixed hydrogen/air combustion at lean to ultra-lean conditions and catalytic approach to enhance stability. *Int. J. Hydrogen Energy* **2023**, *48*, 18100−18115.
(32) Mantzaras, J. Progress in non-intrusive laser-based measurements of gas-phase thermoscalars and supporting modeling near catalytic interfaces. *Prog. Energy Combust. Sci.* **2019**, *70*, 169−211.
(33) Smith, L.; Karim, H.; Etemad, S.; Pfefferle, W. C. *The Gas Turbine Handbook*; National Energy Technology Laboratory (NETL), U.S. Department of Energy, 2006.
(34) Nur Alam Mondal, M.; Karimi, N.; David Jackson, S.; Paul, M. C. Enhancing the performance of catalysts in turbulent premixed fuel-lean hydrogen/air combustion. *Chem. Eng. Sci.* **2025**, *301*, No. 120747.
(35) Alam Mondal, M. N.; Karimi, N.; David Jackson, S.; Paul, M. C. A platinum-coated staggered reactor to intensify lean hydrogen/air combustion: A large eddy simulation study. *Fuel* **2025**, *381*, No. 133386.
(36) Leu, C.-H.; King, S.-C.; Chen, C.-C.; Huang, J.-M.; Tzeng, S.-S.; Liu, I.-H.; Chang, W.-C. Investigation of the packed bed and the microchannel bed for methanol catalytic combustion over Pt/A12O3 catalysts. *Appl. Catal. A Gen* **2010**, *382*, 43−48.
(37) Afandizadeh, S.; Foumeny, E. A. Design of packed bed reactors: guides to catalyst shape, size, and loading selection. *Appl. Therm Eng.* **2001**, *21*, 669−682.
(38) Nguyen, V. N.; Deja, R.; Peters, R.; Blum, L.; Stolten, D. Study of the catalytic combustion of lean hydrogen-air mixtures in a monolith reactor. *Int. J. Hydrogen Energy* **2018**, *43*, 17520−17530.
(39) Ghermay, Y.; Mantzaras, J.; Bombach, R.; Boulouchos, K. Homogeneous combustion of fuel-lean H2/O2/N2 mixtures over platinum at elevated pressures and preheats. *Combust. Flame* **2011**, *158*, 1491−1506.
(40) Deutschmann, O. Modeling of the Interactions Between Catalytic Surfaces and Gas-Phase. *Catal. Lett.* **2015**, *145*, 272−289.
(41) Pashchenko, D. Pressure drop in the thermochemical recuperators filled with the catalysts of various shapes: A combined experimental and numerical investigation. *Energy* **2019**, *166*, 462−470.
(42) Pashchenko, D.; Eremin, A. Heat flow inside a catalyst particle for steam methane reforming: CFD-modeling and analytical solution. *Int. J. Heat Mass Transf* **2021**, *165*, No. 120617.
(43) Moghaddam, E. M.; Foumeny, E. A.; Stankiewicz, A. I.; Padding, J. T. Fixed bed reactors of non-spherical pellets: Importance of heterogeneities and inadequacy of azimuthal averaging. *Chemical Engineering Science: X* **2019**, *1*, No. 100006.
(44) Shahamiri, S. A.; Wierzba, I. Modeling catalytic oxidation of lean mixtures of methane−air in a packed-bed reactor. *Chemical Engineering Journal* **2009**, *149*, 102−109.
(45) Younis, L. B. Modelling of hydrogen oxidation within catalytic packed bed reactor. *Journal of the Energy Institute* **2006**, *79*, 222−227.
(46) Wang, Y.; Zeng, H.; Banerjee, A.; Shi, Y.; Deutschmann, O.; Cai, N. Elementary Reaction Modeling and Experimental Characterization on Methane Partial Oxidation within a Catalyst-Enhanced Porous Media Combustor. *Energy Fuels* **2016**, *30*, 7778−7785.
(47) Azatyan, V. V.; Petukhov, V. A.; Prokopenko, V. M.; Timerbulatov, T. R. Possible Gravitational Stratification of Components in Mixtures of Reaction Gases. *Russian Journal of Physical Chemistry A* **2019**, *93*, 986−987.
(48) Appel, C.; Mantzaras, J.; Schaeren, R.; Bombach, R.; Inauen, A.; Kaeppeli, B.; Hemmerling, B.; Stampanoni, A. An experimental and numerical investigation of homogeneous ignition in catalytically stabilized combustion of hydrogen/air mixtures over platinum. *Combust. Flame* **2002**, *128*, 340−368.
(49) Sui, R.; Mantzaras, J. Combustion stability and hetero-/homogeneous chemistry interactions for fuel-lean hydrogen/air mixtures in platinum-coated microchannels. *Combust. Flame* **2016**, *173*, 370−386.
(50) HELLSING, B. Kinetics of the hydrogen-oxygen reaction on platinum. *J. Catal.* **1991**, *132*, 210−228.
(51) Verheij, L. K.; Hugenschmidt, M. B. On the mechanism of the hydrogen−oxygen reaction on Pt(111). *Surf. Sci.* **1998**, *416*, 37−58.
(52) Argyle, M.; Bartholomew, C. Heterogeneous Catalyst Deactivation and Regeneration: A Review. *Catalysts* **2015**, *5*, 145−269.
(53) du Preez, S. P.; Jones, D. R.; Warwick, M. E. A.; Falch, A.; Sekoai, P. T.; Mota das Neves Quaresma, C.; Bessarabov, D. G.; Dunnill, C. W. Thermally stable Pt/Ti mesh catalyst for catalytic hydrogen combustion. *Int. J. Hydrogen Energy* **2020**, *45*, 16851−16864.
(54) Kozhukhova, A. E.; du Preez, S. P.; Shuro, I.; Bessarabov, D. G. Development of a low purity aluminum alloy (Al6082) anodization process and its application as a platinum-based catalyst in catalytic hydrogen combustion. *Surf. Coat. Technol.* **2020**, *404*, No. 126483.
(55) Kozhukhova, A. E.; du Preez, S. P.; Bessarabov, D. G. Catalytic Hydrogen Combustion for Domestic and Safety Applications: A Critical Review of Catalyst Materials and Technologies. *Energies (Basel)* **2021**, *14*, 4897.

https://doi.org/10.1021/acs.energyfuels.5c00576
Energy Fuels 2025, 39, 9121−9133